

# Numerical Simulation of Rotating Stall in Low Specific Speed Centrifugal Pump Impeller

NGUYEN Xuan-linh, LAI Huan-xin

Key Laboratory of Pressurized Systems and Safety, Ministry of Education, East China University of Science and Technology, Shanghai 200237, China

## ABSTRACT

Rotating stall, a phenomenon that causes flow instabilities and pressure hysteresis, can occur in centrifugal impellers, mixed impellers, radial diffusers, or axial diffusers. Based on the steady-state numerical simulation, this article will analyze the impact of the phenomenon of rotating stall to the flow field in low specific speed centrifugal pump impeller at off-design condition ( $Q=0.25Q_d$ ), where unstable flow most likely occurs, coupled with the standard  $k-\epsilon$  turbulence model. Results show that the significant differences are revealed between the two adjacent impeller passages. One passage is dominated by rotational effects causing high velocities along the blade pressure side (passage A). The other passage (passage B) exhibits a highly separated flow field; the other passage exhibits a highly separated flow field; in the entry section a significant stall is observed, blocking the entry and as the through-flow consequently is minimal, a relative eddy develops in the remaining part of the passage. The flow field and turbulence behavior of steady turbulence flow in the centrifugal pump impeller can be calculated close for steady RANS method, standard  $k-\epsilon$  model. Comparisons are made with experimental results and show good agreement.

**Keywords:** Numerical Simulation, Centrifugal Pump Impeller, Rotating Stall, Off-Design Condition, Standard  $K-\epsilon$

## 1. INTRODUCTION

In recent years, many studies have investigated rotating stall in centrifugal pumps [1-6]. Sinha *et al.* [2] and Guleren *et al.* [4] concluded that stall onset is caused by the separation of leakage flow in the gap between the impeller and the diffuser in centrifugal pumps, according to numerical studies and experimental measurements. Sano *et al.* [3] found that flow instabilities occur in a vaned diffuser with several kinds of stall patterns in a centrifugal pump, and that the onset flow rate of the rotating stall depends on the clearance between the impeller and the diffuser vanes, based on the numerical method. Krause *et al.* [5] and Pedersen *et al.* [8] investigation of rotating stall at different flow rates in a radial pump using time-resolved particle imaging velocimetry (PIV) and Laser Doppler Velocimetry (LDV). The results show the capability of the measuring system of capturing the stall phenomenon and thus allowing its systematic investigation. Byskor *et al.* [7] the flow field in a shrouded six-bladed centrifugal pump impeller has been investigated using large eddy simulation (LES). The stall phenomenon has been to provide detailed flow analysis of flow inside at off-design condition ( $Q=0.25Q_d$ ). However, these are limited knowledge or understanding of rotating stall and the standard  $k-\epsilon$  model is a most general turbulence model especially in centrifugal pump impeller, but it is very rarely used to study stall in centrifugal pump impeller passages. Therefore, in this study, based on the steady-state numerical simulation validated by experimental data with the Standard  $k-\epsilon$  turbulence model has been employed to study the rotating stall in low specific speed centrifugal pump impeller. Meanwhile, the internal

flow in the impeller channels is investigated in terms of the velocity distribution on the different surface. In addition, the turbulence distribution on the different surfaces is also discussed for the impeller passage flow analysis. Based on the aforementioned results, the rotating stall mechanism of the low specific speed centrifugal pump impeller is revealed, thus providing a reference for improving the instability of low specific speed centrifugal pumps.

## 2. NUMERICAL SIMULATION MODELING

Pump Impeller in this study is a shrouded, low-specific-speed pump impeller (shown in Fig. 1). It is scaled from impeller of an industrial multistage pump [8]. The numerical study is taken with a partial load condition ( $Q = 0.25Q_d$ ) in this paper, Pederson [9] has studied the flow by PIV and LDV measurements with two passages.

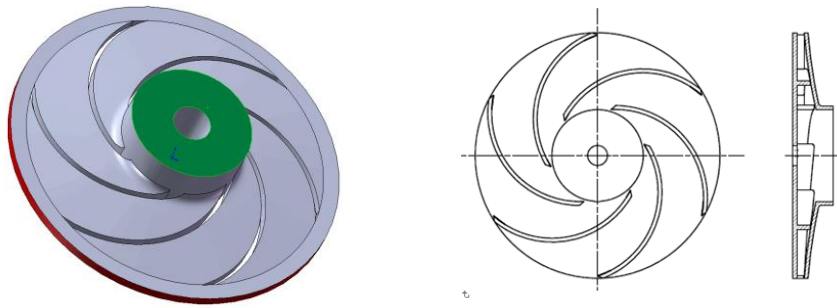


Fig. 1 3D model, Blade-to blade and meridional view of the impeller [9]

The simulation has been done with Fluent 6.3, steady governing equations can be written as following:

$$\begin{cases} \nabla \cdot \mathbf{u}_R = 0 \\ \nabla \cdot (\mathbf{u}_R \otimes \mathbf{u}_R) + 2\boldsymbol{\Omega} \times \mathbf{u}_R + \boldsymbol{\Omega} \times \boldsymbol{\Omega} \times \mathbf{r} = -\nabla \left( \frac{p}{\rho} \right) + \nu \nabla \cdot \nabla \mathbf{u}_R \end{cases} \quad (1)$$

where  $\mathbf{u}_R$  is flow velocity in rotating frame,  $\boldsymbol{\Omega}$  rotating frame speed,  $\mathbf{r}$  position vector,  $p$  fluid pressure,  $\rho$  fluid density, and  $\nu$  the kinematic viscosity.

Turbulence model is important for simulation. The k-epsilon two-equation models use the gradient diffusion hypothesis to relate the Reynolds stresses to mean velocity gradients and the turbulent viscosity. And the k-epsilon models assume that the turbulence viscosity is linked to the turbulence kinetic energy and dissipation via the relation. The Standard k-epsilon model that is widely used in related studies and is suitable for the present study.

The 3D models of impeller were produced by software SolidWorks. The mesh required for the calculations were generated and checked by using the CFD pre-processing package, Gambit. Due to the geometry of the pump impeller is very complex, unstructured mesh is used. EquiAngle Skew and EquiSize Skew of the grid were all less than 0.95, so the grid quality is good. Like the Pederson [10], in this study, the computational domain is not uniform for passage, "two channel". The grid number of computational domain of the impeller is 1510148 in this case. Fig. 2 shows the computational domain and mesh structure.

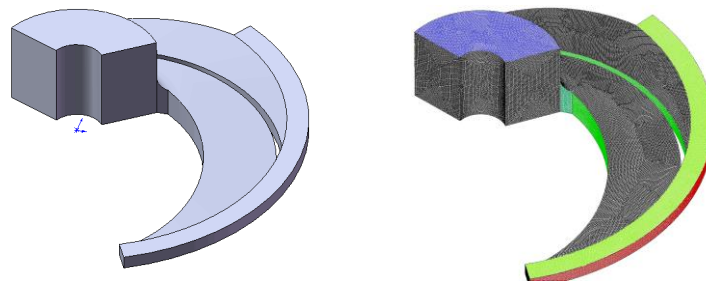


Fig. 2 Computational domain and mesh structure of the impeller

### 3. RESULTS AND DISCUSSION

To ease the discussion it has shown advantageous to distinguish between two impeller passages modeled, which are denoted passage A and B.

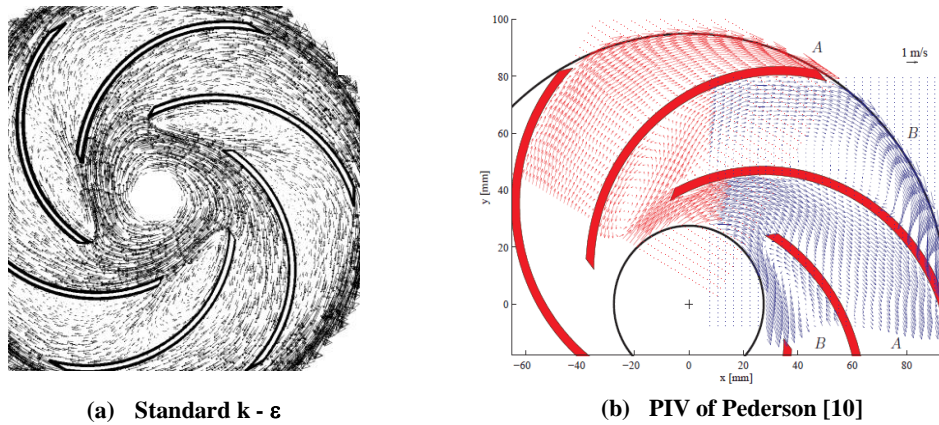


Fig. 3 Vector maps of the relative velocity (W)

3.1. Flow field

Like the PIV results of Pederson for two passage, the flow in the impeller at  $Q = 0.25Q_d$  is not uniform the passages, "two channel" A and B phenomenon consisting of alternate stalled

and unstalled passages has been captured with impeller simulation for Standard  $k - \epsilon$  model as show in Fig. 3. There no difference for two kinds of methods: Standard  $k - \epsilon$  models and PIV the velocity field in impeller from the view at the impeller mid-height ( $z=0.5b_2$ ).

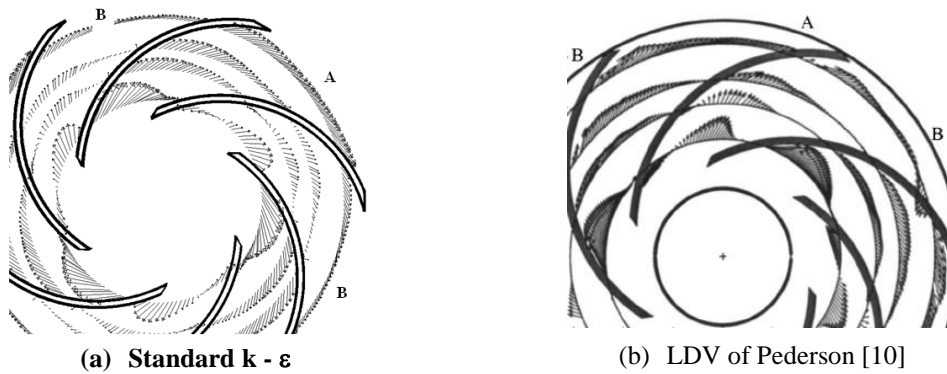
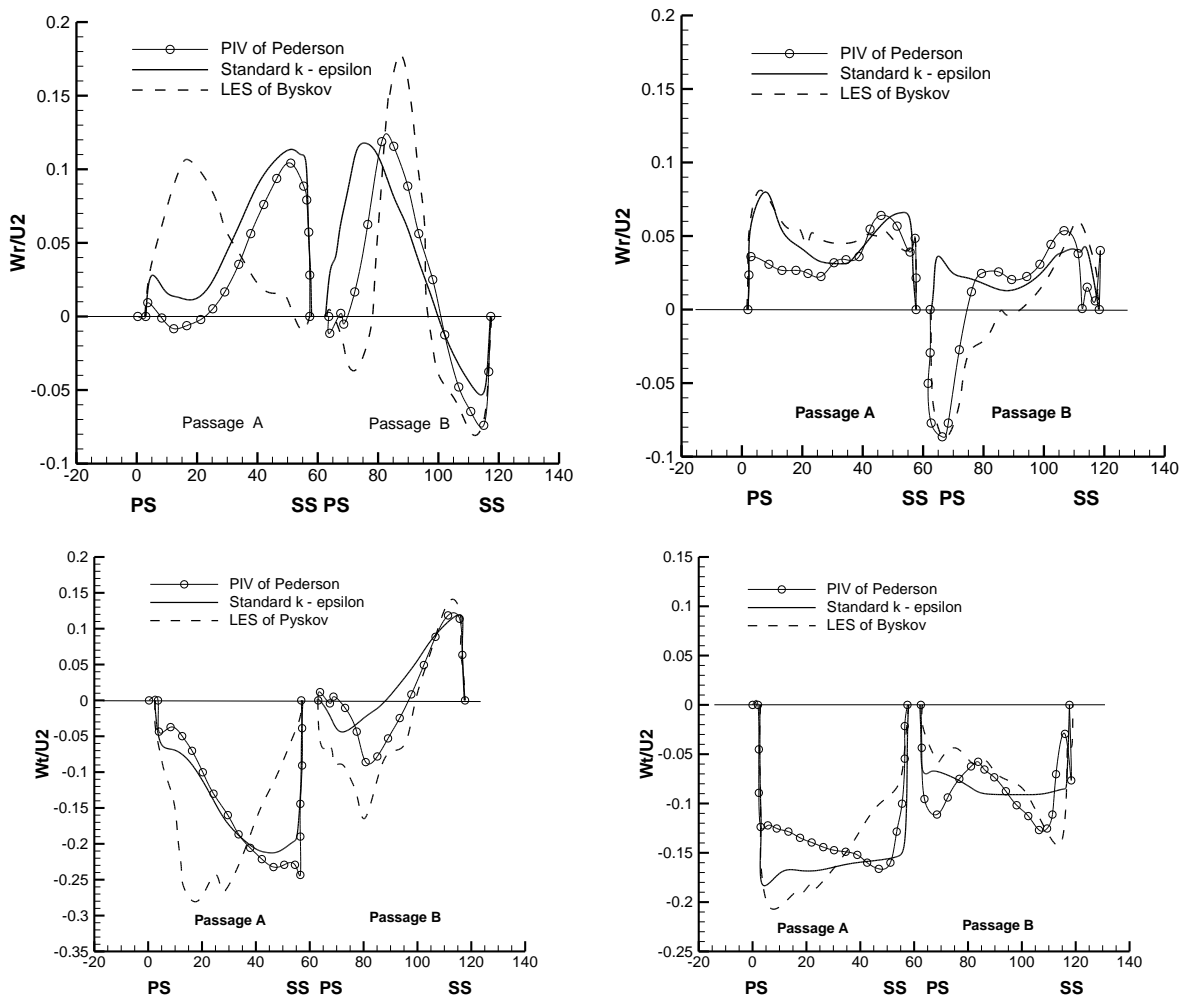


Fig. 4 Vector plots of the relative velocity (W) at radial stations of  $r/R_2=\{0.50, 0.65, 0.75, 0.90\}$

See Fig. 4, the comparisons of the relative velocity (W) at radial stations of  $r/R_2=\{0.50, 0.65, 0.75, 0.90\}$  are taken between simulation results and LDV measurements of Pederson for this case. The comparison of Standard  $k - \epsilon$  model and LDV illustrates that a flow field which is significantly different in the two passages is present. In passage A a relatively well-behaved non separated flow is observed in both Standard  $k - \epsilon$  model and LDV. In passage B the stall in the inlet section is evident and both Standard  $k - \epsilon$  model and LDV shows substantial velocity variations across the passage span at  $r/R_2=0.5$ . Also the relative eddy developing in the remaining part of passage B is clearly present in both Standard  $k - \epsilon$  model and LDV.

$Q/Q_d=0.25, r/R_2=0.5$

$Q/Q_d=0.25, r/R_2=0.9$



**Fig. 5 Radial (top) and tangential (bottom) velocities in the impeller mid-height,  $z/b_2=0.5$ , at radial position of  $r/R_2=0.5$  (left) and  $r/R_2=0.9$  (right)**

Fig.5, comparisons of blade to blade distribution of time average radial and tangential velocities in the impeller mid-height ( $z/b_2=0.5$ ) at radial position of  $r/R_2=\{0.5, 0.9\}$  are also taken between the CFD results, LES of Byskov and PIV measurements of Pederson.

In the inlet section,  $r/R_2=0.5$ , see Fig. 5 (left), the Standard  $k-\epsilon$  turbulence modeling method used in this work do well in calculating velocity profile compared with PIV result, in passage A skewed towards the suction side and this is a huge difference compared to when using large eddy method to study this problem (such the calculation results of Byskov-the velocity profiles displaced to the pressure side [7]). In passage B the stall phenomenon is clearly in the velocity profiles obtained by Standard  $k-\epsilon$ , LES and PIV showing substantial variations across the passage span. The radial and tangential velocities illustrate reversed flow along the suction side and the Standard  $k-\epsilon$ , LES and PIV are seen to agree.

At,  $r/R_2=0.9$ , Fig. 5(right), calculation results compared with LES and PIV not much difference, radial velocity profiles are observed to become relatively flat in passage A [7]. The PIV measurements reveal velocity profiles in passage A skewed towards the suction side,

whereas with Standard  $k-\epsilon$  and LES in contrast to this. In the passage B, the calculation result is observed to predict the variation in the radial velocity, but the phenomenon of reverse flow does not exist. Meanwhile, in both the LES and PIV radial velocities give evidence of the relative eddy with positive velocities along the suction side and reversed flow along the pressure side [7]. The variations between the calculation result and both the LES and PIV are relatively larger when analysis the tangential velocity.

3.1. Turbulence behavior

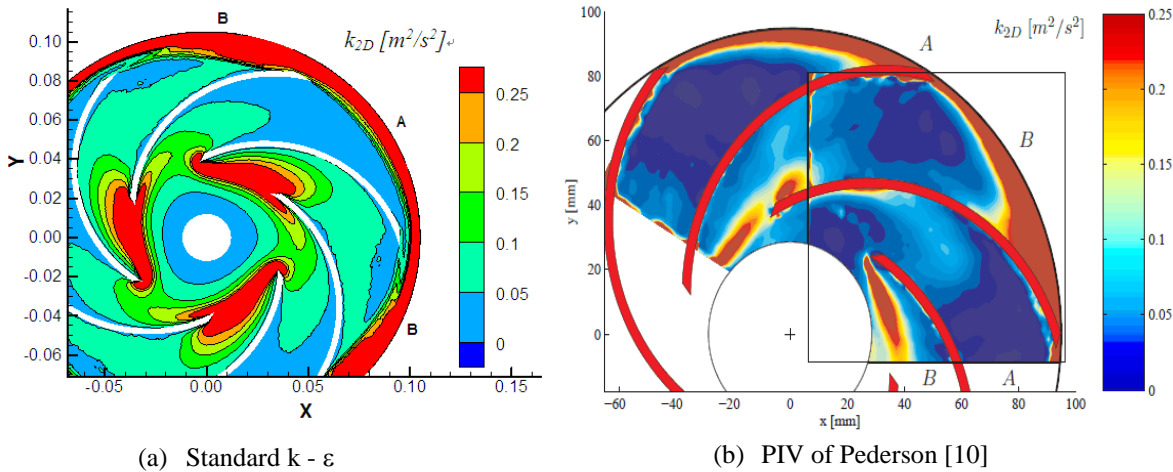


Fig. 6 Contour plots of the Turbulent kinetic energy ( $k_{2D}$ ) in the impeller mid-height,  $z/b_2=0.5$

From Fig. 6 (a), It is very clearly that the largest turbulent kinetic energy ( $k_{2D}$ ) is in the impeller outlet and inlet part of stalled passage (passage B). In the passage B, a high turbulent kinetic energy ( $k_{2D}$ ) flow could be found starting from trailing edge of suction side, and stopping at the pressure side of this passage. This is not found in passage A (unstalled passage). Compared with PIV (Fig. 6 b), the results are quite similar.

The comparisons of blade to blade distribution of turbulence intensity (Tu) are given in Fig. 7 for radial position  $r/R_2=0.5$  and  $r/R_2=0.98$ . At  $r/R_2=0.5$ , the Tu predicted by Standard k-ε from pressure side to suction side in both passage larger than its PIV. Especially in the near of pressure side in stalled passage B, the calculation value of Tu is the largest-7% and

the value predicted by PIV is about 50% smaller than Standard k-ε.

At the  $r/R_2=0.98$ , the PIV has got a “V” type profil for Tu with the higher Tu in pressure side than suction side for both passage and larger than Standard k-ε. Meanwhile, the Tu predicted by Standard k-ε decline from pressure side to suction side and value of Tu is the largest-11% in stalled passage B.

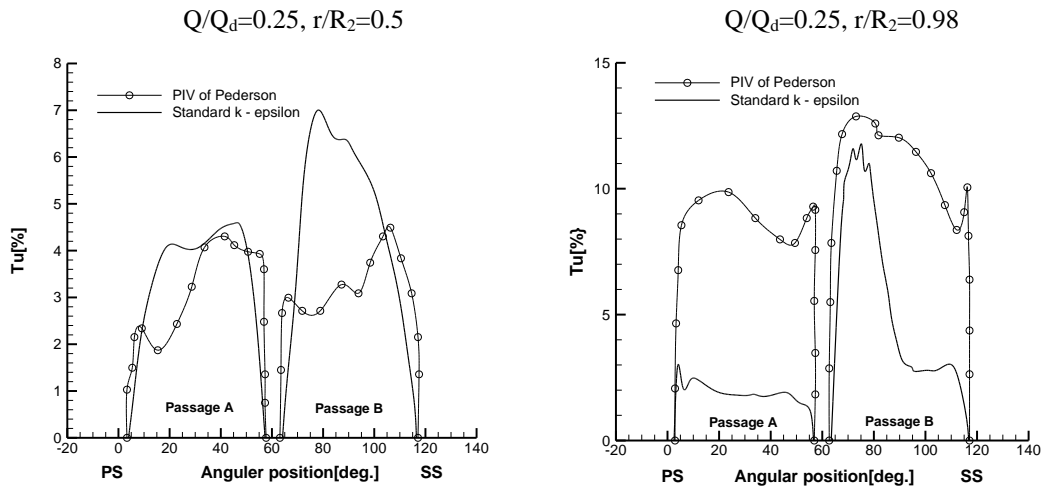


Fig. 7 Blade to blade distribution of turbulence intensity (Tu) in the impeller mid-height,  $z/b_2=0.5$ , at radial position  $r/R_2=0.5$ (left) and  $r/R_2=0.98$ (right)

4. CONCLUSION

Numerical simulations has been carried out investigate the performance instability of flow in centrifugal pump impeller. Results were compared with experimental results.

Standard k - ε model is a most general turbulence model especially in centrifugal pump impeller. However, it is very rarely used to study stall in centrifugal pump impeller passages at partial load condition (off-design condition).

From above discussing, the significant differences are revealed between the two adjacent impeller passages. One passage is dominated by rotational effects causing high velocities along the blade pressure side (passage A). The other passage (passage B) exhibits a highly separated flow field; the other passage exhibits a highly separated flow field; in the entry section a significant stall is observed, blocking the entry and as the through-flow consequently is minimal, a relative eddy develops in the remaining part of the passage. The flow field and turbulence behavior of steady turbulence flow in the centrifugal pump impeller can be calculated close for steady RANS method, standard  $k-\epsilon$  model, and has compared for PIV result of reference paper.

## REFERENCES

- [1] Hergt P, Starke J. Flow patterns causing instabilities in the performance curves of centrifugal pumps with vaned diffusers. In: *Proceedings of the second international pump symposium*, Texas, (1985), pp. 67–75 .
- [2] Sinha M, Pinarbasi A, Katz J. The flow structure during onset and development states of rotating stall within a vaned diffuser of a centrifugal pump. *J Fluids Eng*, (2001), 123(3):490–499.
- [3] Sano T., Yoshida T., Tsujimoto Y., et al.. Numerical study of rotating stall in a pump vaned diffuser. *J Fluids Eng*. (2002), 124(2): 363-367.
- [4] Guleren KM, Pinarbasi A. Numerical simulation of the stalled flow within a vaned centrifugal pump. *J Mech Eng Sci*. (2004), 218(4):425–435.
- [5] Krause N., Zahringer K., Pap E. Time-resolve particle imaging velocimetry for the investigation of rotating stall in a radial pump. *J Experiments in Fluids*. (2005), 39:192-201.
- [6] Lucius A, Brenner G. Numerical simulation and evaluation of velocity fluctuations during rotating stall of a centrifugal pump. *J Fluids Eng*. (2011), 133(8):0811021–0811028.
- [7] Byskor R.K., Jacobsen C. B., Pedersen N. Flow in a centrifugal pump impeller at design and off-design condition-Part I: Large eddy simulation. *ASME J. Fluid Eng*. (2003), 125:73-83.
- [8] Grundfos A. S.: *WinCAPS Catalogue*. Ver 7.0. Product No: 41260001 CR4-20/1, (1997).
- [9] Pedersen N., Larson P.S., et al.: Flow in a centrifugal pump impeller at design and offdesign conditions-Part I: Particle Image Velocimetry (PIV) and Laser Doppler Velocimetry (LDV) measurements. *ASME J. Fluid Eng*. (2003), 125: 61–72.